

Capacitive frost depth indicator

V. Papez¹ and S. Papezova^{2,*}

¹Czech Technical University in Prague, Faculty of Electrical Engineering, Department of Electrotechnology, Technická 2, CZ166 27 Pague 6, Czech Republic

²Czech University of Life Sciences in Prague, Faculty of Engineering, Department of Electrical Engineering and Automation, Kamycka 129, CZ165 21 Prague 6 - Suchdol, Czech Republic

*Correspondence: papezovas@tf.czu.cz

Abstract. The depth of soil freezing, i.e., the depth at which water is frozen, is a significant factor in meteorology, as it affects many processes in agriculture, building, etc. Soil frost penetration is an important factor for overwintering organisms, but also for physical and chemical processes in soil, particularly for its mechanical properties. The depth of freezing is normally determined directly, i.e. mechanically, using a special soil freezing meter, i.e., frost-depth indicator, according to the process of water freezing in the probe. Another method lies in determining the soil temperature by the interpolation of the curves from the graph, as measured by soil thermometers according to the change in the resistivity of soil or water, when frozen. The principle of the frost-depth indicator function is to evaluate the temperature dependence of water permittivity, which decreases, when water is frozen, from $\epsilon_r \sim 87$ at $1\text{ }^\circ\text{C}$ to $\epsilon_r \sim 3.2$ at $-1\text{ }^\circ\text{C}$, typical for ice. The water permittivity is evaluated by a measuring capacitor, which is adapted into the shape of the frost depth indicator probe, whose dielectric is deionized water. During freezing, the capacity is reduced in this area. The capacity of the partially frozen probe is directly proportional to the length of its non-frozen section. The measuring capacitor is a part of the resonant circuit of the oscillator. The frequency of the oscillator varies with the capacity of the probe and is further evaluated. The achievable measurement accuracy is approximately 2% for the probe of a 1m length and in direct evaluation by an autonomous counter. For the computer evaluation, with the possibility to compensate the probe non-linearity, the measurement accuracy is approximately 0.5%.

Key words: depth of soil freezing, capacity measurement, water permittivity.

INTRODUCTION

The depth of soil freezing is currently measured in many ways. The easiest method is to use a mechanical indicator, which is a hose filled in with distilled water. The hose is inserted into a plastic pipe that is permanently embedded in the soil. The depth of soil freezing is evaluated by the operator's palpation of the hose after a couple of hours after inserting the probe into the soil. The non-frozen section appears soft, while the frozen section is hardened, which indicates the presence of ice (Pokladníková et al., 2005). Similarly, the freezing depth is evaluated by means of a soil monolith. Here, a soil

sample is used as a probe medium, whose state is again evaluated by the operator (Střelcová & Škvarenina, 2005)

Other methods evaluate the depth of freezing according to soil temperature. In the methods using thermometers, temperature readings from the thermometers, which are embedded at different depths in soil, are evaluated. According to the temperature course samples, the position of the temperature function passing through zero is then approximated and a freezing depth is assigned to this position.

More advanced designs use temperature indications for substance, whose colour considerably varies with certain temperatures. The frost depth indicator is a probe containing a substance that significantly changes its colour around 0 °C. The frost depth indicator is inserted into soil. After temperature stabilization and subsequent removal of the probe, the depth of soil freezing is evaluated according to the position of the colour transition in the probe. Electrical measurements exploit the changes in resistivity of soil or water, when frozen. The resistivity of frozen water and soil is by several orders higher than the resistivity of non-frozen water and soil.

Frost depth indicators evaluating the soil-freezing depth according to the soil resistivity use the probe, made of the insulator with separated electrodes on the surface. Electrical resistance is then measured in between them. The probe is inserted into soil and the depth of freezing is determined by the position of the electrodes, where the resistance sharply increases (Bagal, 2010a, Bagal, 2010b).

The methods employing the change in water resistivity during freezing work in a similar way, with the only difference that the water filling and the electrodes are enclosed inside the probe, inserted into the soil.

A mechanical procedure is the most used procedure for its simplicity and reliability. Its disadvantage, the same as at other non-electrical processes, is the need for the operator's manipulation with the device at the measuring station, which excludes a remote measuring of the depth of freezing. On the other hand, electrical procedures usually allow remote measurements. However, their disadvantage is the undesirable influence of conductivity measurements of the non-frozen electrolyte or soil between the electrodes and the surface states of the electrodes, on which the evaluated resistance strongly depends. These phenomena then complicate the evaluation of the measurement, which is complex and may be unreliable.

The capacitive frost depth indicator, described below, works on the principle of the evaluation of water permittivity, which decreases at the high-frequency range from $\epsilon_r \sim 87$ (at 1 °C) to $\epsilon_r \sim 3.2$ (at -1 °C), at the temperature typical for ice (Chaplin, 2017).

Water permittivity is evaluated by a measuring capacitor that is adapted into the shape of the frost depth indicator, vertically embedded into soil. When the part of the probe freezes, the capacity of the measuring capacitor is reduced in this area and the total capacity of the probe decreases. The total probe capacity varies between the minimum value, corresponding to the fully frozen probe, and the maximum value, corresponding to the non-freezing probe.

In order to achieve high measurement accuracy, both the probe construction and the capacity evaluation method are optimized with respect to the parasitic capacity parameters of the measuring capacitor and the frequency dependence of the complex water permittivity (Artemov & Volkov, 2014).

MATERIALS AND METHODS

The measuring probe is principally designed as a plate capacitor, whose dielectric is distilled water, or ice and other suitable solid and flexible dielectric (Papež, 2013). An example of a possible design of the probe is shown in Fig. 1, in a sectional view, perpendicular to the longitudinal axis of the probe.

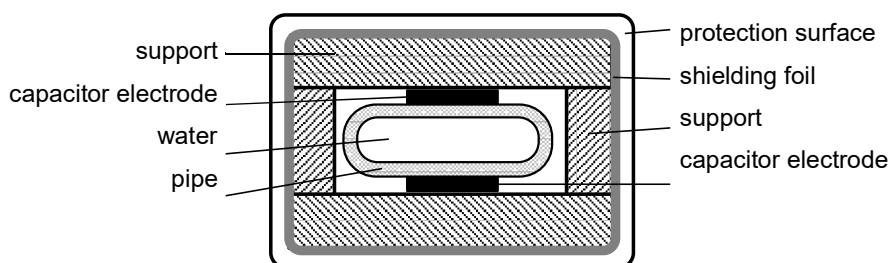


Figure 1. Example of a measuring probe design.

The basis of the probe design is formed by two strips thin conductive metallic foils, serving as measuring capacitor electrodes which are glued and attached to two rigid plates made of high-quality solid dielectrics. Both plates are mechanically interconnected and fixed by means of two rigid dielectric rectangular constructions. In this way a rectangular hollow is formed along the whole length of the probe between the plates and dielectric construction, on whose opposed walls are located the electrodes of the measuring capacitor. A flexible tube, made of low-loss dielectric, is inserted into the hollow along the full length of the probe. The tube is filled in, under moderate overpressure, with airless distilled water and hermetically sealed. The tube has, in terms of the probe function, three important functions:

- a) reduces the impact of a large increase in permittivity; and, if need be, of a water loss factor during de-freezing, on the properties of the measuring capacitor;
- b) allows suppressing the occurrence of any electrochemical processes on the surface of the electrodes placed in water by separating the water filling from the electrodes by an inert dielectric layer;
- c) prevents the mechanical construction of the probe from degradation and damage, caused by the increase in volume of the water filling during freezing. The change in volume of water is hereby compensated by the compression of the flexible material of the tube, in which the water filling is closed.

From the outside, the probe is shielded with a thin metallic foil, which is glued on the outer sides of the plates, or is mounted on the sides of the probe, and it is connected to the film on the outside of the dielectric plates. The protection against the external influence/impact is ensured by coating the probe with a plastic tube, resembling a hose. The capacity frequency dependencies of the probe sample and its loss factor ($D = 1/Q$) are shown for a non-frozen probe (Fig. 2), and a frozen probe (Fig. 3). Length of a probe sample was selected at 1 m. As a material for the tube, a silicone rubber with a wall thickness of 1 mm was used. The width of measuring capacitor plates was 6 mm and water channel height was 4 mm.

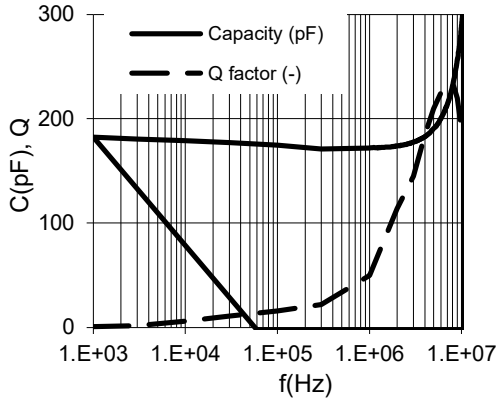


Figure 2. The capacity frequency dependence and Q factor for a non-frozen probe.

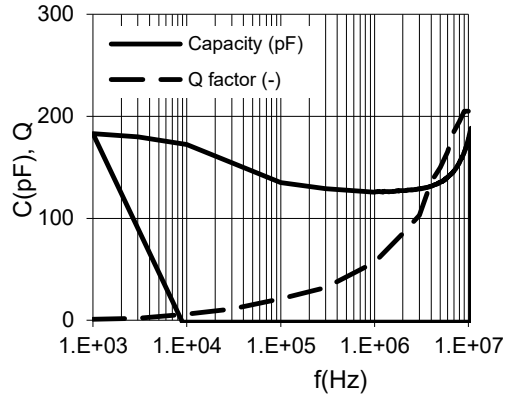


Figure 3. The capacity frequency dependence and Q factor for a frozen probe.

The change in capacity of the probe, when frozen, is best seen in the frequency range of 0.3–3 MHz, where the capacity of a non-frozen probe (with the leads) is 181 pF and the capacity of a frozen probe is 135 pF. At frequencies lower than 30 kHz (Artemov & Volkov, 2014), the capacity of the frozen probe is significantly influenced by the polarization of ice at temperatures around $-1\text{ }^{\circ}\text{C}$. A sharp rise in its permittivity to the values corresponding to liquid water, also results in the increase in the capacity of a frozen probe, in the low frequency range, to the values, corresponding to the frozen probe. At the same time, at low frequencies, the loss factor of the capacitor, representing the probe, increases significantly. These phenomena exclude the possibility of using of conventional commercial capacity meters, operating in the low frequency range at frequencies from 100 Hz to 100 kHz for capacity measurement.

At higher frequencies, the capacity of the non-frozen probe is influenced by its internal inductance and inductance of the leads. Reactance of the serial inductance reduces capacitor reactance at high frequencies, resulting in a fictitious increase in its capacitance and an increase in its loss factor. Assuming the frost depth evaluation according to the capacity ratio of the frozen and partially frozen probes, the phenomenon also complicates the measurement because the indicated ratio of fictitious capacity reactance does not correspond to the desired ratio of real capacity reactance

$$\frac{X_{C1} - X_L}{X_{C2} - X_L} \neq \frac{X_{C1}}{X_{C2}} \quad (1)$$

where X_{C1} – reactance of a non-frozen probe; X_{C2} – reactance of a frozen probe; X_L – reactance of probe inductance.

To achieve the accuracy in measuring the probe capacitance, it is best to use the frequencies around 3 MHz, where the capacitor has low losses, the quality factor $Q > 100$ and the influence of the probe inductance still remains very small.

Since only commercially available high-performance measuring instruments, such as HP 4291, Agilent 4285, or Keysight E4991, allow measuring in this frequency range, a special device for evaluating the probe capacity has been designed and implemented.

The probe capacity is evaluated by the frequency of an RF oscillator, in whose resonant circuit the measuring capacitor is inserted. The principal diagram of the oscillator is shown in Fig. 4. The resonance frequency of the control circuit, which is depends on the probe freezing length is determined by Eq. (2)

$$f = \frac{1}{2\pi} \frac{1}{\sqrt{L(C_0 + C_k) - L\Delta Cl}}, \quad (2)$$

where L – inductance of a resonant circuit; C_0 – total capacity of a non-frozen probe, including leads; ΔC – proportional drop in capacity of the probe, when frozen; C_k – capacitance of a calibration capacitor; l – the ratio of the length of the probe frozen section to the total length of the probe measuring section, $0 \leq l \leq 1$.

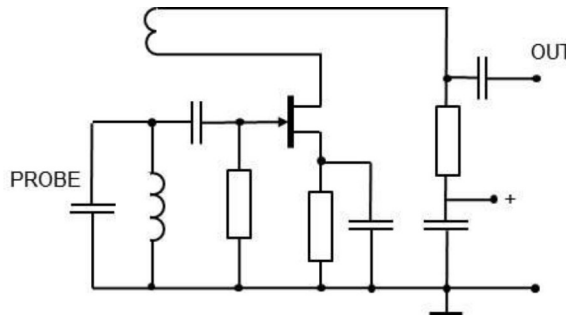


Figure 4. Principal diagram of the oscillator.

Considering the fact that, for a non-frozen probe, $l=0$, the resonance frequency is f_0 , for small changes in frequency, using the approximation $(1+x)^{-0.5} \approx 1-x/2$, f can be exactly (2) or approximately, expressed by Eq. (3).

$$f = f_0 \frac{1}{\sqrt{1 - \frac{\Delta C}{(C_0 + C_k)} l}} \approx f_0 \left(1 + \frac{\Delta C}{2(C_0 + C_k)} l\right) \quad (3)$$

According to the approximating formula, the length of the frozen section of the probe, depending on the resonant frequency f , can be expressed by a simple linear function

$$l = \left(\frac{f}{f_0} - 1\right) \frac{2(C_0 + C_k)}{\Delta C}. \quad (4)$$

The error caused by the inaccuracy of the approximation is small for small values of the ratio $\Delta C/(C_0+C_k)$, or for the ratio f_i/f_0 of the oscillation frequencies with a frozen and non-frozen probe. The error increases with the increasing value of these ratios. The size of the maximum error, resulting from the approximation can be, according to the fore mentioned ratio $\alpha = f_i/f_0$, expressed by

$$\text{MAX}(l - l_A) \leq \frac{\frac{\sqrt{2}\alpha}{\sqrt{\alpha^2 + 1}} - \frac{\alpha}{2} - \frac{1}{2}}{\alpha - 1}. \quad (5)$$

In contrast, the measurement error, resulting from the frequency instability of the measuring oscillator and its temperature dependence with the increasing ratio of α ,

decreases and the resulting error in determining the relative freezing time reaches approx. $\delta f/(\alpha-1)$, depending on relative frequency deviation δf . Both these dependencies are shown in the graph in Fig. 5.

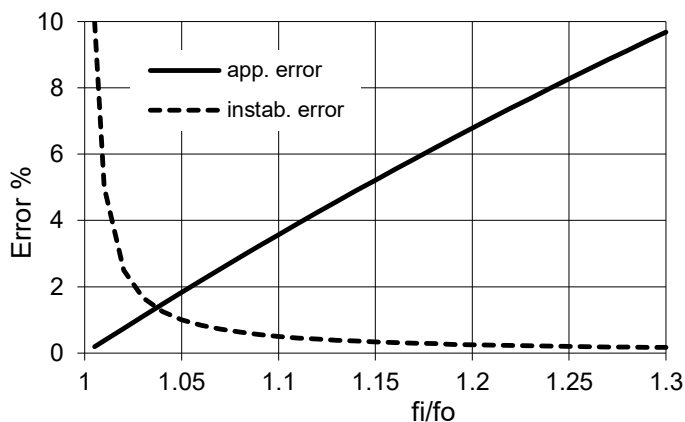


Figure 5. Error dependence caused by the approximation and the error caused by frequency instability at $\alpha=f_i/f_0$.

Function (4), expressing the length of the frozen section, depending on the frequency of the measuring oscillator signal, is evaluated by a counter, whose input signal is a measuring oscillator signal. In the counter operation algorithm, the coefficient $C_0/\Delta C$ can be set by selecting the counting time, and the differential operation is realized by resetting the counter in its overflow. The counter module M and the counting time T are selected so that, in processing the signal f_0 with the non-frozen probe, the counter should overflow at least once during the counting period and the number indicated after the counting should equal zero (6).

$$T = \frac{Mn}{f_0} = \frac{Mn + A}{f_i} . \quad (6)$$

When the water has been frozen, the indicated number corresponds to the difference between the just generated frequency f_j , and the frequency f_0 , with a non-frozen probe. If the ratio of f_j/f_0 and the counter module are suitably chosen, using (5), both the counting time and the number of counter overflows during the counting period n can be determined such that the number indicated at the counter output directly corresponds to the length A of the probe freezing. A is expressed in appropriate length units ($A \leq M - 1$).

RESULTS AND DISCUSSION

Following the results of the above mentioned analysis, a sample of a frost depth indicator with a direct indication of the depth of freezing has been designed. A probe of a 1m length, having the capacity of 135 pF in a frozen state and 181 pF in a non-frozen state has been applied. The construction of the oscillator is based on the principle diagram shown in Fig. 4.

A principal diagram of the frost depth indicator is shown in Fig. 6. The resonant circuit of the oscillator is completed by an adjustable capacitor C_A . An inductor L of the resonant circuit has an adjustable inductance.

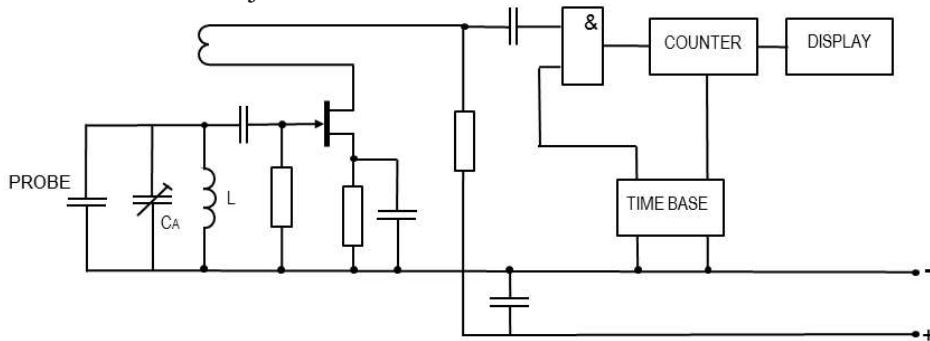


Figure 6. Principal diagram of the frost depth indicator.

By adjusting the adjustable elements, the oscillator operating frequencies f_0 and f_i are set to the appropriate selected values, corresponding to the applied counter algorithm, as specified by (Chaplin, 2017). The frequency of the measuring oscillator is evaluated by a counter, whose resulting state is displayed on the display, after the counting has been finished. The counting period and counter timing are controlled by the time base circuit.

For the sample of the frost depth indicator were selected $f_0 = 3.2$ MHz and $f_i = 3.4$ MHz, and the module 1,600 ($16 \cdot 100$). The counter overflows at the moment, when the counting time reaches $500 \mu\text{s}$ at a non-frozen probe. When the probe of a 1 m length freezes, the counter enables direct indication of freezing in the value range of 0–100. The values correspond to the freezing length in centimeters. The realized frost depth indicator is shown in Fig. 7.



Figure 7. Realized frost depth indicator.

When the measurement is evaluated by a computer, a digital signal depicting the indicated frequency is sent to a computer, where the length of freezing is either computed according to exact mathematical relations or is read from the conversion table. The data for the conversion table can be most easily obtained by calibrating the sensor. In this way, it is possible to consider all the phenomena that influence the measurement without any further errors.

Measurement accuracy can be further increased by introducing a correction of the temperature dependence of the oscillator on its operating temperature. The method is suitable for long-distance evaluation of measurements from many sensors through the

measurement center because the sensors are simple and the signal can be transmitted over a long distance.

The frost depth indicator was tested in a mode close to its real use in practice. The probe was partially inserted into a space with a temperature of approx. $-5\text{ }^{\circ}\text{C}$ and the device together with the second part of the probe were placed in a heated box, whose temperature was maintained at about $5\text{ }^{\circ}\text{C}$. The probe was slipped through the hollow and fixed in such a way to let freeze only its selected length. The readings of the values were carried out in a steady state, i.e., 8–16 hours after the last manipulation with the device. Comparative measurements were carried out after the probe was partially inserted into a heated box with the temperature of $5\text{ }^{\circ}\text{C}$, and the device together with the second part of the probe were inserted into the space with the temperature of $-5\text{ }^{\circ}\text{C}$.

The results of the test are shown in Fig. 8 and Fig. 9. A measurement error of 1.6% of the maximum value was detected in the middle of the measuring range. The error resulted from the simplification of the evaluation algorithm by a linear approximation. The shift by $10\text{ }^{\circ}\text{C}$ of the operating temperature of the measuring device causes an error of the indicated value by approximately 1%.

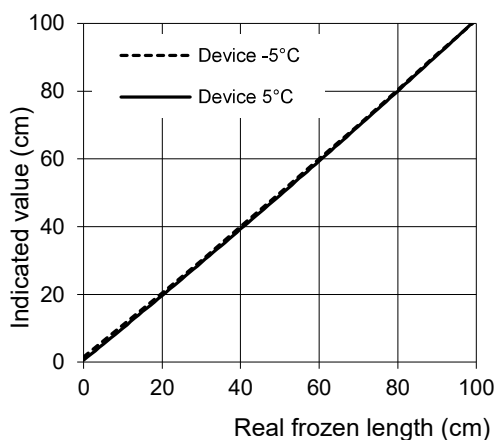


Figure 8. Dependence of the indicated value on the actual length of a frozen part.

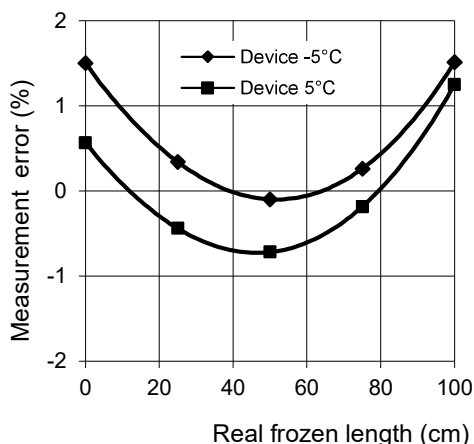


Figure 9. Dependence of the measurement error on the length of a frozen part.

CONCLUSIONS

The capacity probe for the soil freezing depth evaluation has been designed to achieve the maximum mechanical and electrochemical stability of the probe. The analysis of the frequency dependence of the probe complex impedance has been carried out. Based on its results, the method of the probe capacity evaluation has been determined, which allows to achieve the highest accuracy of the measurement.

With respect to the loss factor and parasitic inductance of the capacitor representing the probe, the optimum frequency range of 2–3 MHz was determined to evaluate the probe capacity. The principle of its evaluation is to monitor the resonance frequency of the resonant circuit, whose part is also the probe. The resonant circuit serves, at the same time, as an oscillator control circuit, whose operating frequency enables the evaluation of the requested capacity.

When the frequency is directly evaluated by the counter, the accuracy of the freezing depth measurement is approximately 2%. When the frequency is evaluated by the microcomputer, the accuracy can be improved to approx. 0.5%, when using the compensation of parasitic influences.

ACKNOWLEDGEMENTS. Thanks for cooperation belong to Laboratory of Faculty of Electrical Engineering, Czech Technical University in Prague and Department of Electrical Engineering and Automation, Faculty of Engineering, Czech University of Life Sciences in Prague.

REFERENCES

- Artemov, V.G. & Volkov, A.A. 2014. Water and Ice Dielectric Spectra Scaling at 0 °C. *Ferroelectrics* **466**, 158–165.
- Bagal, Z. 2010a. Electronic soil freeze meter. Patent. Office of Industrial Property. Patent document 2010–286 (in Czech).
- Bagal, Z. 2010b. Electronic soil freeze meter. Utility design. Office of Industrial Property. Patent document 2010-22559 number of registration 21177 (in Czech).
- Chaplin, M. 2017. Water and Microwaves. *Water structure and science*. http://www1.lsbu.ac.uk/water/microwave_water.html. Accessed 30.12.2017.
- Papež, V. 2013. Soil freeze meter. Patent. Office of Industrial Property. Patent document 304000. 2013-06-26. (in Czech).
- Pokladníková, H., Rožnovský, J. & Dufková, V. 2005. Soil freezing at the station Bystrice nad Perštejnem, In: *Bioclimatology of present and future*, Krtiny, ISBN 80-86 690-31-08 (in Czech).
- Střelcová, K. & Škvarenina, J. 2005. *Bioclimatology a meteorology*. Technical University in Zvolen, 138 pp. (in Slovak).